

Numerical Study Of Flow In Asymmetric 2D Plane Diffusers With Different Inlet Channel Lengths


 Open
Access

 Muhammad Tukur Hamisu^{1,*}, Mahmud Muhammad Jamil¹, Umar Sanusi Umar¹, Aisha Sa'ad¹
¹ Department of Mechanical Engineering, Faculty of Engineering, Nigerian Defence Academy, PMB 2109, Kaduna, Nigeria

ARTICLE INFO

ABSTRACT

Article history:

Received 23 January 2019

Received in revised form 7 April 2019

Accepted 11 May 2019

Available online 20 May 2019

In this paper, flow in asymmetric 2D diffusers with different inlet channel lengths (Model 1 and Model 2) by using various turbulence models (k-epsilon, k-omega and SST k-omega) was studied, and the trends in the two different inlet channel lengths were compared. In order to study separation and assess the effectiveness and consistency of different CFD turbulence models, primarily two models of asymmetric 2D diffusers were designed accordingly. The trend of the velocity profiles for the two models followed that of the experiment. The turbulence models used k-omega and SST k-omega for both models have shown separation of boundary layer is more significant in stations $x/H = 14$, and $x/H = 24$. Also, in station $x/H = 34$ where flow is fully developed, the standard k-epsilon turbulence model shows better performance as compared to other turbulence models. Moreover, separation was under predicted by k-omega and SST k-omega in model 2 due to sudden decrease in flow velocity because of its shorter inlet channel length as compared to model 1. The different turbulence models for the two models can be represented in terms of decreasing order of Y^+ values as follows : k-epsilon > SST k-omega > k-omega.

Keywords:

 Asymmetric 2D plane diffuser,
 turbulence models, different inlet
 channel lengths

Copyright © 2019 PENERBIT AKADEMIA BARU - All rights reserved

1. Introduction

Nowadays, high performance computers enable engineers to simulate complex geometries computationally by solving couple of partial differential equations (PDE) for momentum, continuity and energy equations numerically using one of present Computational Fluid Dynamics (CFD). CFD codes are powerful and are common in industries and yield satisfactory results. Generally, CFD has become the central of comprehension fundamentals of fluid flow processes, such as fluid-flow, heat-transfer, mass transport, and have recently found applications in medical fields.

In this paper, turbulent flow in an asymmetric 2D diffuser with different inlet channels is studied. In many applications, knowing whether the boundary layer (laminar or turbulent by calculating the Reynolds Number which is the ratio of the inertia force to viscous force of a fluid flow) will separate from the surface or inside a specific body is important. If it occurs, it is also important to know

* Corresponding author.

E-mail address: mt.hamisu@nda.edu.ng (Muhammad Tukur Hamisu)

precisely where flow separation will occur. The separation could be internally or externally [1]. This is quite important in many design problems.

Flow separation occurs when the boundary layer travels far enough against an adverse pressure gradient that the speed of the boundary layer relative to the object falls practically to zero [2,3]. The fluid flow becomes detached from the surface of the object, and as a result takes the forms of eddies and vortices. The boundary layer detaches from the surface into a broader wake. The boundary layer closest to the wall or leading edge reverses in flow direction. The point between the forward and backward flow is called the Separation Point, where the shear stress is zero. Initially, the overall boundary layer thickens rapidly at the separation point and is then forced off the surface by the reversed flow at its bottom [4].

Cebeci *et al.*, [5] accurately calculated the separation points in incompressible turbulent flows using four prediction methods Goldschmied's, Stratford's, Head's and the Cebeci-Smith's method and then validated them experimentally. Knob *et al.*, [6] studied the dynamics of boundary layer separation using the Time-Resolved PIV and Bi-Orthogonal decomposition technique to study the rapid structure of the separation region, its development and coherent structures theoretically and the simple case of adverse pressure gradient experimentally. Gustavsson [7] and Yang *et al.*, [8] experimentally studied flow separation using a high-resolution Particle Image Velocimetry (PIV) system to study the rapid structure of the separation region, its development and the reattachment of the turbulent flow and the results were compared to conventional measurements using static pressure taps [8], hot-wire anemometer and a Preston tube. Chandavari *et al.*, [9] investigated flow separation in a planar diffuser by varying the diffuser taper angle for axisymmetric expansion in order to delay the separation. Tornblom *et al.*, [10] experimentally and numerically studied a new separation flow control approach by means of streamwise vortices.

Flows through backward facing step, asymmetric or sudden expansion geometries are of importance from the viewpoint of fundamental fluid mechanics and many practical applications due to the fact that all the complexities of separation and reattachment of turbulent flow in the presence of adverse pressure gradient can be captured therein [11-13]. The turbulent fluid flows through asymmetric geometry or sudden expansion duct are common in numerous engineering applications such as combustors, aircrafts, pipelines, nuclear reactors, turbo-machineries heat exchangers, bluff buildings etc. [12,13].

Buice and Eaton [14] experimentally studied flow through an asymmetric plane diffuser, and their diffuser has so far received a lot of acceptance as the benchmark.

Numerically, there have been numerous researches in understanding flow in an asymmetric plane diffuser using different turbulence models. Berdanier [13] first employed the one-equation Spallart-Almaras equation for its simplicity, followed by the two equation models studied ($k-\epsilon$, $k-\omega$) and then the five equation Reynolds Stress Model. Salehi *et al.*, [15] employed low Re $k-\epsilon$, the $k-\omega$, the $V^2 - f$ and a variant of Reynolds stress model. Similarly, Kumar and Kabbur [16] used $k-\epsilon$, $k-\omega$ and included $k-\epsilon$ Re-Normalisation Group (RNG). Firstly, Elbehery [14] and Laccarino [17] used low Re $k-\epsilon$, the $k-\omega$ and then further employed User Defined Scalars and User Defined Routines. In a similar study, Jamil *et al.*, [18] concluded the possibility of using the turbulence models as applied to flow in rectangular channels with baffle plates. All the models agreed very close to the experimental work. In another study, Saqr *et al.*, [19] numerically studied confined vortex flow using modified the $k-\epsilon$ turbulence model. The modified $k-\epsilon$ turbulence model shows better performance compared to RNG $k-\epsilon$ and Standard $k-\epsilon$ model.

Obi *et al.*, [20] experimentally and computationally studied separation in an asymmetric plane diffuser and their work has received wide attention. Others who have studied this phenomenon both

experimentally and computationally include Klistafani [21] and Tornblom [22] and their results were in agreement with the two methods when compared.

To the authors' knowledge, no investigation has been made on flow in the standard Buice and Eaton asymmetric two-dimensional diffuser with different inlet channel lengths. Therefore, the objective of this study is to numerically analyze flow asymmetric two-dimensional diffusers with different inlet channel lengths by using various turbulence models and compare the trends between the two different inlet channel lengths.

The findings of this study will further the literatures in understanding turbulence, separation, reattachment and suitable implementation of turbulence models which are important in designing practical engineering applications.

2. Methodology

2.1 Mathematical Formulations and Computational Methods

This study employed steady Reynolds Averaged Navier-Stokes equations (RANS) outlined in Eq. (1), Eq. (2) and Eq. (3) via the ANSYS FLUENT 16.2 software package. The governing RANS equation is given by:

$$\frac{\partial u_i}{\partial x_j} = 0 \quad (1)$$

$$\frac{\partial u_i \partial u_j}{\partial x_j} = -\frac{1}{\rho} \frac{\partial P}{\partial x_i} + \frac{\partial}{\partial x_j} (V S_{ij} \overline{u'_i u'_j}) \quad (2)$$

Where S_{ij} is the main strain rate and it is calculated by:

$$S_{ij} = \frac{1}{2} \left(\frac{\partial u_i}{\partial x_j} + \frac{\partial u_j}{\partial x_i} \right) \quad (3)$$

and $\overline{u'_i u'_j}$ is the unknown turbulent or Reynolds-stress tensor and u'_i represents the velocity fluctuation in i – direction. These equations are not a closed set and turbulence models are required to model the turbulence or Reynolds-stress tensor.

For all the simulations, a two-dimensional, double-precision flow solver was used. The application of steady RANS equations was assumed to be sufficient for this study because the flow through the diffuser is steady in the mean.

It is worth mentioning that there are two other numerical methods of solving turbulence, namely: Direct Numerical Simulation (DNS) and Large Eddy Simulation (LES). These modeling techniques have increased complexities and deemed unnecessary to resolve the flow properties of interest.

2.2 Turbulence Models

Three turbulence models (k - ϵ k - ω and SST k - ω) are employed to predict the flow behaviour in a planer asymmetric diffuser. The turbulence models are based on the Boussinesq hypothesis in Eq. (4). In which the Reynolds stress tensor is derived from the effective viscosity formulation, which is a direct extension of the laminar deformation law. It is given by:

$$\tau_{ij} = \frac{2}{3} k \delta_{ij} - 2\nu_t S_{ij} \quad (4)$$

Where, $k = \overline{u'_i u'_j}$ is the turbulent kinetic energy, δ_{ij} is the Kronecker delta and ν_t denotes turbulent kinematic viscosity. In order to obtain the turbulent viscosity, other transport equations are needed. These equations differ and have advantages and disadvantages from one model to another.

2.2.1 Standard k-epsilon (k-ε)

This model is one of the most commonly used turbulence model. This model employs the Boussinesq hypothesis and includes two additional partial differential transport equations: One for the turbulent kinetic energy, k , and one for the dissipation, ϵ . The main advantage of the $k-\epsilon$ model is its completeness no information about mixing length or distance to the nearest wall is required [23]. In the derivation of the $k-\epsilon$ model, it is assumed that the flow is fully turbulent, and the effects of molecular viscosity are negligible. Thus, the standard $k-\epsilon$ model is valid for fully turbulent flows only [24]. Jones and Launder [25] originally developed the standard $k-\epsilon$ model.

$$\frac{\overline{Dk}}{Dt} = \nabla \cdot \left(\frac{\nu_t}{\sigma_k} \nabla k \right) + P - \epsilon \quad (5)$$

$$\frac{\overline{D\epsilon}}{Dt} = \nabla \cdot \left(\frac{\nu_t}{\sigma_\epsilon} \nabla \epsilon \right) + C_{\epsilon 1} \frac{P\epsilon}{k} - C_{\epsilon 2} \frac{\epsilon^2}{k} \quad (6)$$

$$\nu_t = C_\mu \frac{k^2}{\epsilon} \quad (7)$$

Where P is a production term [23].

Further definition of the $k-\epsilon$ model employed the default model constants on ANSYS FLUENT:

$$C_\mu = 0.09 \quad C_{\epsilon 1} = 1.44 \quad C_{\epsilon 2} = 1.92 \quad \sigma_k = 1.0 \quad \sigma_\epsilon = 1.3$$

2.2.2 Standard k-omega (k-ω)

The standard $k-\omega$ model is one of the widely used turbulence models and also employs the Boussinesq hypothesis. The turbulent properties of the flow and represented by two additional transport equations. Full derivations for the closure equations are provided by Wilcox [26]. The governing equation derived by Wilcox is:

$$\frac{\overline{D\omega}}{Dt} = \nabla \cdot \left(\frac{\nu_t}{\sigma_\omega} \nabla \omega \right) + C_{\omega 1} \frac{P\omega}{k} - C_{\omega 1} \frac{P\omega}{k} - C_{\omega 2} \omega^2 \quad (8)$$

The first transported variable is turbulent kinetic energy, k , similar to the turbulent kinetic energy equation of the standard $k-\epsilon$ model. The second is the specific dissipation, ω , which can also be thought of as the ratio of ϵ to k . The model combines modifications for low-Re effects, compressibility and shear flow spreading. Pope [23] conducted an exercise to derive the ω -equation from the ϵ -equation, taking $\sigma_k = \sigma_\epsilon = \sigma_\omega$:

$$\frac{\overline{D\omega}}{Dt} = \nabla \cdot \left(\frac{\nu_t}{\sigma_\omega} \nabla \omega \right) + (C_{\epsilon 1} - 1) \frac{P\omega}{k} - (C_{\epsilon 2} - 1) \omega^2 + \frac{2\nu_t}{\sigma_\omega k} \nabla \omega \cdot \nabla k \quad (9)$$

Therefore, for inhomogeneous turbulence, the equations are not the same since the ϵ -equation written in terms of in Eq. (9) which contains an additional term.

For the Standard $k-\omega$ model, the default model constants on ANSYS FLUENT were used:

$$\alpha_{\infty}^* = 1.0 \quad \alpha_{\infty} = 0.52 \quad \beta_{\infty}^* = 0.09 \quad \beta_i = 0.072 \quad \gamma^* = 1.5$$

The $k-\omega$ model is agreed to be as a useful turbulence model for wall-bounded flows such as the channelled diffuser used in this study. More importantly, the $k-\omega$ model is capable of determining the wall shear stress for most flows, thus making it a suitable choice for investigating the separation in this asymmetric diffuser.

2.2.3 Shear-Stress Transport (SST $k-\omega$)

The SST $k-\omega$ model was developed by Menter [27], which combines the capabilities of the $k-\varepsilon$ model away from the walls and robustness of $k-\omega$ turbulence model near the walls. The definition of the turbulent viscosity is modified to account for the transport of turbulent shear stress. The model equations are provided in

$$\nu_t = \frac{a_1 k}{\max\left\{a_1 \omega, \frac{\partial u}{\partial y} F_2\right\}} \quad (10)$$

where F_2 is a function of the flow specifically:

$$F_2 = \begin{cases} 1 & \text{for boundary layers} \\ 0 & \text{for free shear layers} \end{cases} \quad (11)$$

For the Standard $k-\omega$ model, the default model constants on ANSYS FLUENT were used:

$$\alpha_{\infty}^* = 1.0 \quad \alpha_{\infty} = 0.52 \quad \beta_{\infty}^* = 0.09 \quad \gamma^* = 1.5 \quad M_{t0} = 0.25 \quad a_1 = 0.31 \quad \beta_i^{inner} = 0.075$$

$$\beta_i^{outer} = 0.0828 \quad \sigma_k^{inner} = 1.176 \quad \sigma_k^{outer} = 1.0 \quad \sigma_{\omega}^{inner} = 2.0 \quad \sigma_{\omega}^{outer} = 1.168$$

2.3 Problem Description

In this study, the geometry considered for the 2D asymmetric plane diffuser is shown in Figure 1 where the dimension of geometry was according to Buice and Eaton [14]. There are two geometries to be considered that have different inlet channels. An extended inlet channel length (15H) and a short inlet channel length (3H) but other dimensions remain the same between the two geometries.

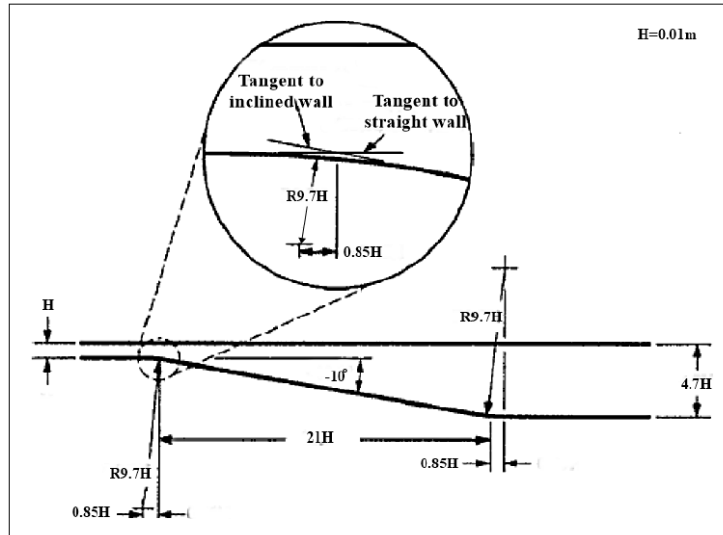


Fig. 1. Buice and Eaton Diffuser [14]

2.3.1 Inlet velocity and other parameters

Assumptions and some important parameters that have been considered for the analysis are given below.

The flow is considered to be incompressible, uniform with the value of U_o at the inlet and Mach number to be lower than 0.3. Where Re is Reynolds Number 20,000, ρ is the density (1.225 kg/m^3), H is the inlet height of the diffuser (0.01m) and μ is the viscosity 1.789×10^{-5} . The density and viscosity values were obtained from properties of air in FLUENT.

The inlet velocity can be calculated from Reynolds Number formula in Eq. (12). By making the velocity U_o subject of the formula its value can be obtained.

$$Re = \frac{\rho U_o H}{\mu} \quad (12)$$

$$U_o = \frac{Re \mu}{\rho H} = \frac{20000 \times 1.789 \times 10^{-5}}{1.225 \times 0.01} = 29.21 \text{ m/s}$$

2.4 Creation of the Models

The design of proposed models of the asymmetric two dimensional diffuser carried out in SolidWorks. By following standard procedure, two models of asymmetric 2D diffuser were created as per required specifications as shown in Figure 2 and 3.

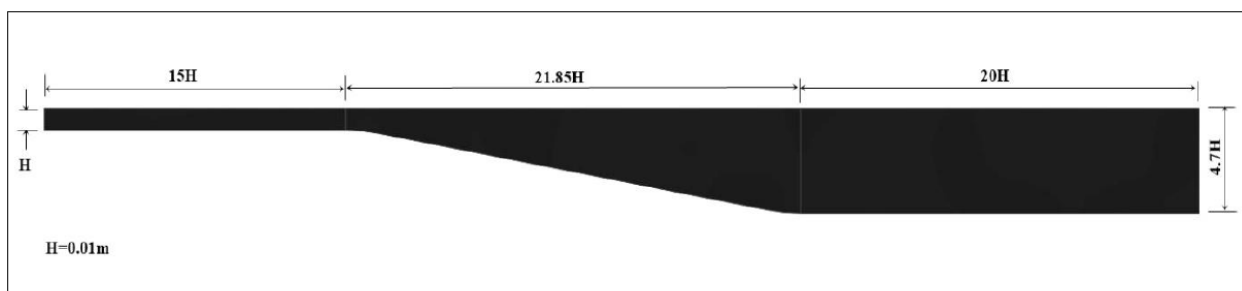


Fig. 2. Model 1 of the 2D asymmetric diffuser (15H inlet channel length)

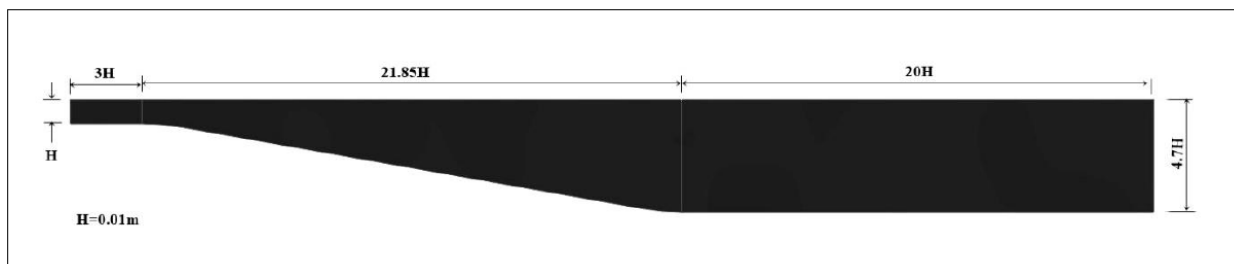


Fig. 3. Model 2 of the 2D asymmetric diffuser (3H inlet channel length)

2.5 Grid or Mesh Generation

The accuracy of any simulation highly depends on the quality of the grid. By considering the physics of the flow, a good quality mesh or grid would lead to faster convergence and better solution. The grid should at least have some grid or mesh quality as defined by measures of orthogonality particularly at the boundaries, grid or mesh skewness, grid spacing, aspect ratio etc. [28,29]

The method used in the grid generation is quite straightforward. Started with a grid of 100 x 30 across the two co-ordinate directions (horizontal and vertical), each grid was made to be significantly finer than the previous grid by doubling the number of grid points in each co-ordinate direction.

2.5.1 Model 1 (15H inlet)

Figure 4 and Table 1 below show the generated mesh and mesh specifications of model 1 with 15H inlet channel.

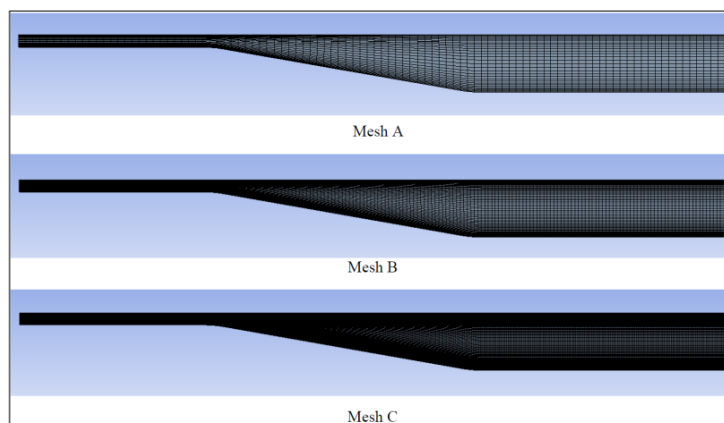


Fig. 4. Generated Mesh Model

Table 1

Mesh Generation Specification Model 1

Grid	No. of Elements	No. Vertical Walls Grids	No. Upper Walls Grid	No. Lower Walls Grids
1(100×30)	3,131	30	27, 37, 36	27, 3, 31, 3, 36
2(200×60)	12,261	60	54, 74, 72	54, 6, 62, 6, 72
3(300×120)	48,811	120	108, 148, 144	108, 12, 124, 12, 144

2.5.2 Model 2 (3H inlet)

Figure 5 and Table 2 below show the generated mesh and mesh specifications of model 2 with 3H inlet channel.

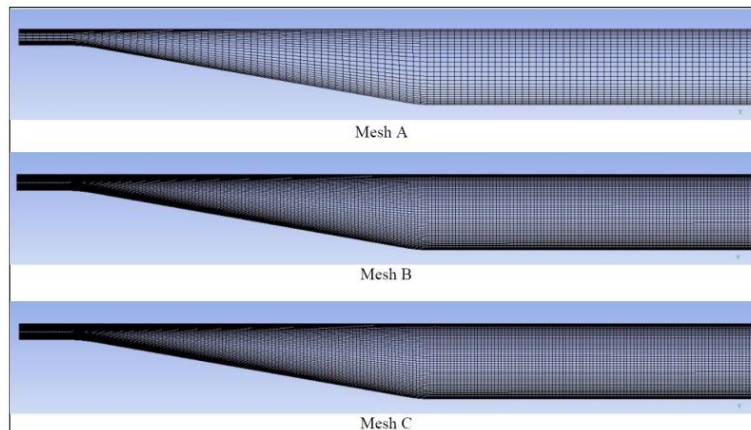


Fig. 5. Generated Mesh Model 2

Table 2
 Mesh Generation Specification Model 2

Grid	No. of Elements	No. Vertical Walls Grids	No. Upper Walls Grid	No. Lower Walls Grids
1(100×30)	3,870	30	7, 48, 45	7, 4, 40, 4, 45
2(200×60)	13,680	60	14, 96, 90	14, 8, 80, 8, 90
3(300×120)	48,160	120	28, 192, 180	28,16,160,16, 180

2.5.3 Quality of the grid/mesh generated

It is always a good practice to check the quality of the grids or mesh generated before running the calculations. Minimum orthogonal quality ranges from 0 to 1, where values close to 0 correspond to low quality. Maximum orthogonal quality skewness ranges from 0 to 1, where values close to 1 correspond to low quality [28,29]. See Table 3 and 4 below.

Table 3
 Model 1 Mesh Quality

Grid/Mesh	Minimum Orthogonal Quality	Maximum Orthogonal Skewness	Maximum Aspect Ratio
1(100×30)	8.382×10^{-1}	1.618×10^{-1}	4.333×10^1
2 (200×60)	7.918×10^{-1}	2.082×10^{-1}	4.318×10^1
3 (300×120)	9.677×10^{-1}	3.240×10^{-2}	4.310×10^1

Table 4
 Model 2 Mesh Quality

Grid/Mesh	Minimum Orthogonal Quality	Maximum Orthogonal Skewness	Maximum Aspect Ratio
1(100×30)	8.622×10^{-1}	2.513×10^{-1}	4.235×10^1
2 (200×60)	8.346×10^{-1}	3.982×10^{-1}	4.253×10^1
3 (300×120)	9.414×10^{-1}	5.865×10^{-2}	4.280×10^1

2.6 Boundary Conditions

The two models (15H and 3H Inlet Channels) were divided into three parts. The first vertical wall is the inlet and set to inflow boundary condition. The last vertical wall is the outlet and set to outflow boundary condition. The upper and lower (horizontal) walls is set to wall boundary condition. The same boundary conditions were employed for all turbulence models.

In Inflow boundary condition, the properties of all flow distribution need to be specified at the inlet, mainly flow velocity. This type of boundary condition is widely employed where the inlet flow velocity is known [30]. In a diffuser, accurate representation of inlet boundary condition is critical for numerical results [31].

In Outflow boundary conditions, the properties of all flow variables have to be specified at outlet boundaries mainly flow velocity. This can be understood in conjunction with inlet boundary condition. This type of boundary condition is widely employed where the inlet flow velocity is known. When the outlet is selected far away from the geometrical disturbances, the flow achieves a fully developed state where there are no changes in the flow direction. In such region, an outlet could be outlined and the gradient of all variables could be equated to zero in the flow direction except pressure [30].

The wall or no-slip boundary condition is the most widely used boundary condition in fluid flow problems. This is the most suitable conditions for velocity components at the wall. The normal component could be directly set to zero whereas the tangential component is set to the velocity of the wall [30].

2.7 Solution Strategy and Convergence

A second-order upwind discretization scheme was used for the momentum equation while a first-order upwind discretization was used for turbulent quantities. Generally, the properties of a numerical scheme are satisfactory accuracy or consistency, stability and convergence were ensured. Caretto *et al.*, [32] Patankar and Spalding [33] and Patankar [34] developed the SIMPLE algorithm defined as used for pressure-velocity coupling. Implicitly, the discretized equations are solved sequentially, starting with the pressure equation, followed by the momentum equations, then the pressure correction equation, and finally the equations for the scalars (turbulence variables). The criterion used for convergence involved the monitoring the values of skin friction and variation of velocity profiles with iteration, and reduction of several orders of magnitude in the residual errors.

2.8 Mesh Independence Study

This is a common practice and it is also known as grid independence or mesh convergence. Successive solutions are obtained on finer and finer grids or mesh until the solution variation from one grid to the next grid approaches an accepted tolerance, the solution is assumed to have converged or approaching the exact solution. The difference between two refinements is usually taken as a measure of the accuracy. The coarse mesh which gives a solution which is invariant with the finer meshes, the grid independence is said to be achieved and that coarse mesh is used for further analysis.

Y plus (Y^+) value also plays an important role in mesh independence study. During each stage of mesh refinement, variation of Y^+ value with the change of mesh size have been evaluated for each case, and it is found that the Y^+ value is decreasing while using finer mesh sizes. Y^+ is a non-

dimensional wall distance for a wall bounded flow. It is widely used in defining the law of the wall and in boundary layer theory and which can be expressed as given below in Eq. (13).

$$y^+ = \frac{u \times y}{\nu} \tag{13}$$

Where u is the velocity due to friction at the nearest wall, y is the distance to the nearest wall and ν is the local kinematic viscosity of the fluid. The Mesh independence study is conducted on the two geometries, with 15H and 3H inlet channels.

2.8.1 Model 1 (15H inlet channel)

The k-epsilon turbulence model is taken in order to check independence of the mesh. For the mesh independence study, any of the four stations can be used to test the convergence. In this case, station of $x/H=6$ and $x/H=14$ and ' y/H ' versus ' U/U_0 ' have been plotted as shown in Figure 6 and 7 and the variation of Y plus value with different grid size can be shown in Table 5 below.

From Figure 6 and 7, it is certain that solutions of the k-epsilon turbulence model of the diffuser is converged and there are no more variant with the finer meshes. Since variation between the solutions of Mesh B and Mesh C is very minute and negligible, therefore coarse Mesh B is going to be considered as standard mesh for rest of the analysis with k-omega and k-omega SST turbulence.

Table 5
 Y+ values for different meshes (Model 1)

Meshes	Y Plus (Y+)
Mesh A	8.7
Mesh B	5.2
Mesh C	2.3

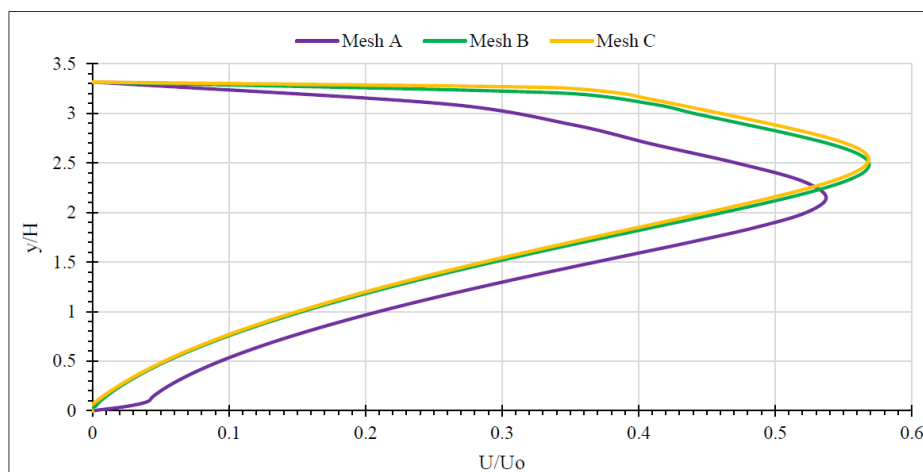


Fig. 6. ' y/H ' versus ' U/U_0 ' for $x/H = 6$ (Model 1)

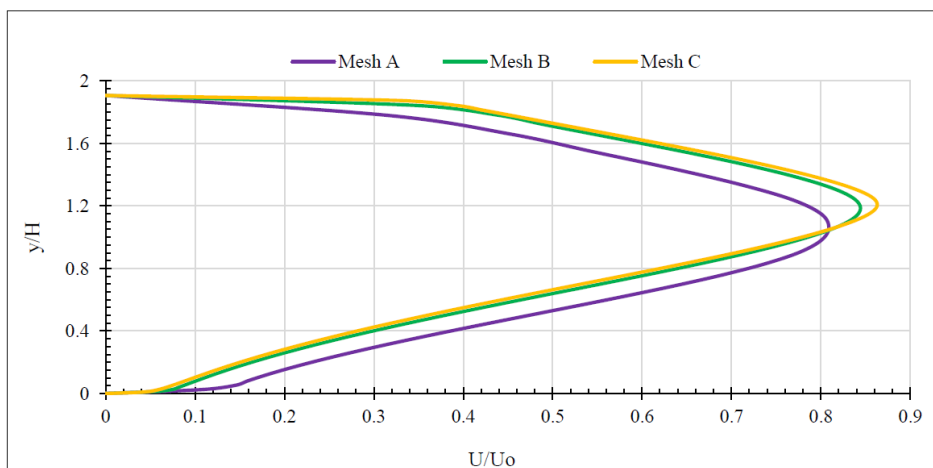


Fig. 7. y/H' versus ' U/U_o ' for $x/H = 14$ (Model 1)

2.8.2 Model 1 (3H inlet channel)

For model 2, same procedure was followed in order to check independence of the mesh using k-epsilon turbulence model; and ' y/H ' versus ' U/U_o ' values were plotted for the stations $x/H=6$ and $x/H=14$ as shown in Figure 8 and 9; and the variation of wall $Y+$ value with different grid size can be seen from the Table 6.

Table 6
 $Y+$ values for different meshes (Model 2)

Meshes	Y Plus ($Y+$)
Mesh A	8.2
Mesh B	4.7
Mesh C	2.7

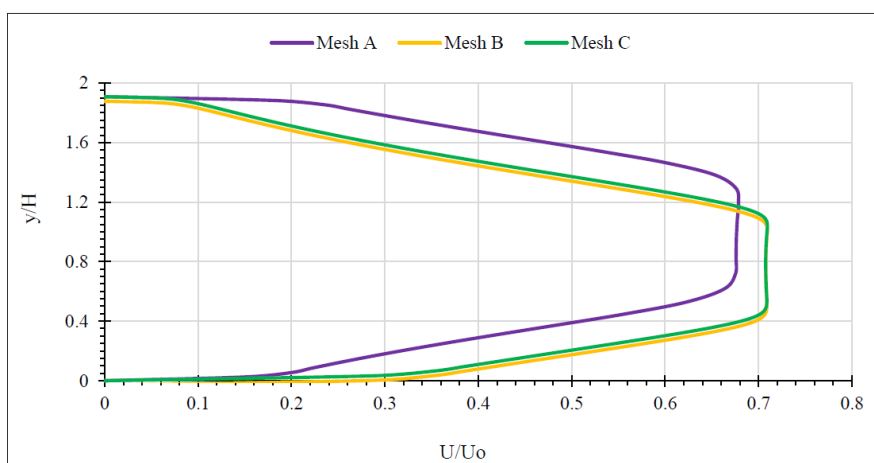


Fig. 8. ' y/H ' versus ' U/U_o ' for $x/H = 6$ (Model 2)

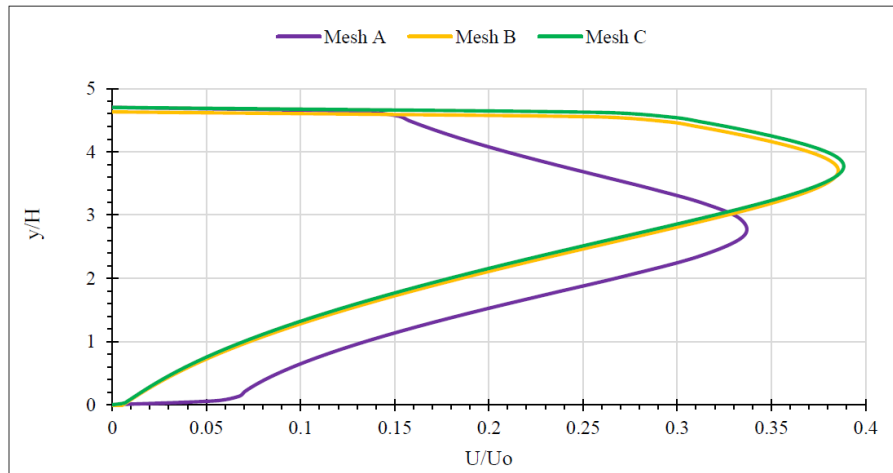


Fig. 9. y/H' versus ' U/U_o ' for $x/H = 14$ (Model 2)

From Figure 8 and 9, it is certain that solutions of the k-epsilon turbulence model of the diffuser is converged and there is no more variation with the finer meshes. In this model coarse Mesh B is considered as standard mesh for rest of the analysis with k-omega and k-omega SST turbulence model of the two dimensional diffuser model, since difference between results of Mesh B and Mesh C is negligible. Therefore, coarse Mesh B is considered as standard mesh for rest of the analysis with k-omega and k-omega SST turbulence model of the two dimensional diffuser model.

3. Results and Discussion

3.1 Analysis of the Asymmetric 2D Diffuser Turbulent Flow

When air enters the expansion section of the diffuser, the flow is separated due to the adverse pressure gradient and a large separation/recirculation region is generated. The CFD simulation results are studied in the expansion section to predict the size of the recirculation bubble and its effect on velocity profiles.

The asymmetric two dimensional diffuser model has been analyzed using Mesh B (for both model 1 and model 2) by means of three different turbulence model viz. standard k-epsilon, standard k-omega and SST k-omega. Detailed presentation and discussion of the numerical results is given below.

3.1.1 Analysis of model 1 (15H inlet channel)

Model 1 was analyzed using mesh B (200x60), for all three turbulence models - standard k-epsilon, standard k-omega and SST k-omega as mentioned above. The contours x-velocity of these models is shown in Figure 10 to 12 showing velocity profiles and separations. From the figures, it can be seen that, inlet of the diffuser possess highest velocity, as the flow goes out from the inlet channel its velocity in x-direction decreases due to increase in area and pressure in the diffuser, and the velocity at the lower wall of the diffuser is minimum (negative velocity at some points). The negative velocity at the lower wall of the 2D asymmetric diffuser represents separation of boundary layer.

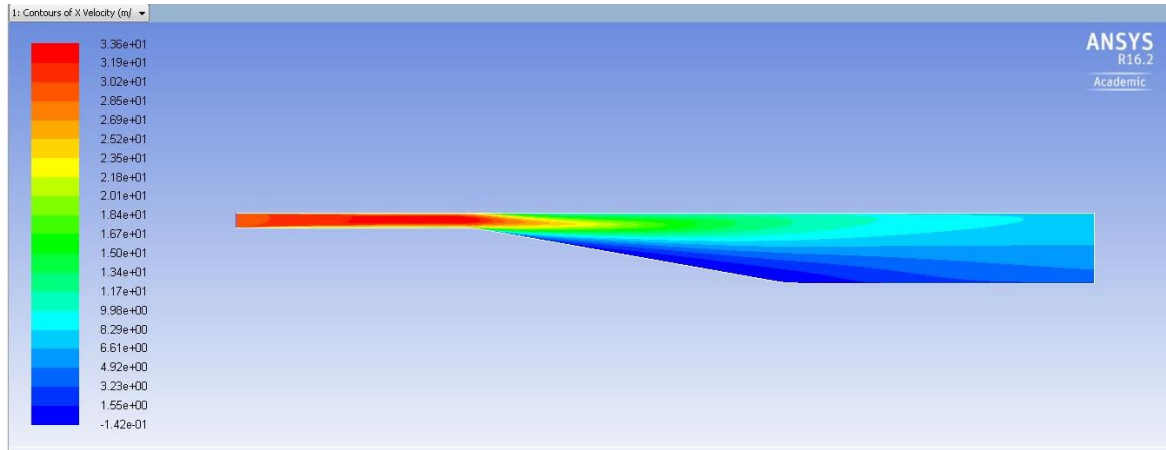


Fig. 10. Contours of X-velocity for the standard k-epsilon turbulence model

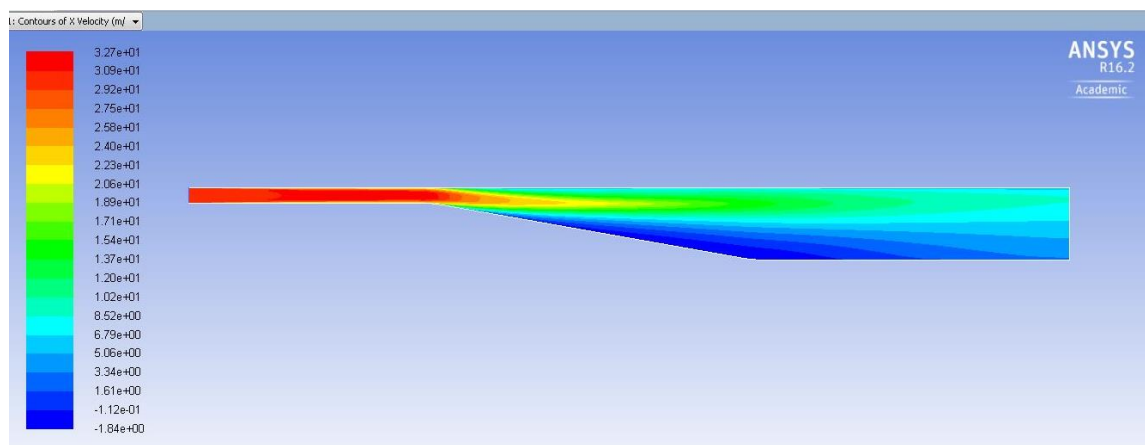


Fig. 11. Contours of X-velocity for the standard k-omega turbulence model

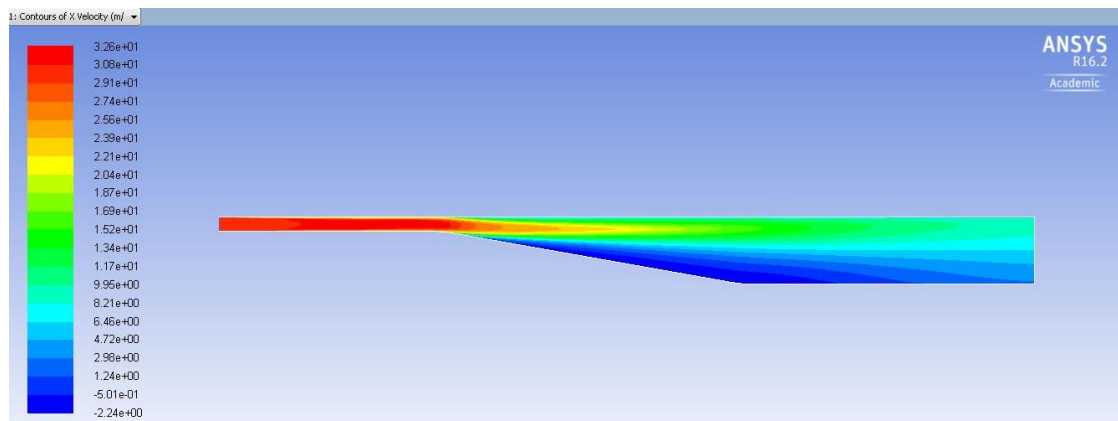


Fig. 12. Contours of X-velocity for the standard SST k-omega turbulence model

Figure 13 represents the Y^+ values for different turbulence models viz. standard k-epsilon, standard k-omega and SST k-omega of the 2D asymmetric diffuser model. From the figure, it is certain that standard k-omega and SST k-omega turbulence models have lower values of wall Y^+ as compared to standard k-epsilon turbulence model.

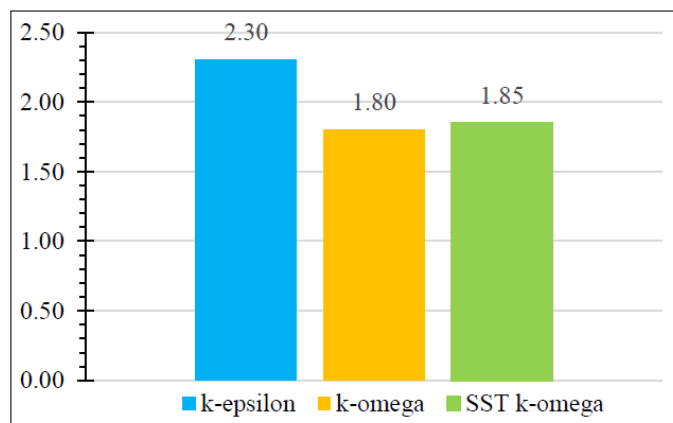


Fig. 13. Y+ values for different turbulence model (Model 1)

The U/U_0 values at different stations or curve lengths namely $x/H = 6$, $x/H = 14$, $x/H = 24$ and $x/H = 34$ measured from the expansion point (as shown in the Figure 14) are compared to the different turbulence models and experimental results of the 2D asymmetric diffuser, and represented from Figure 15 to 17 below.

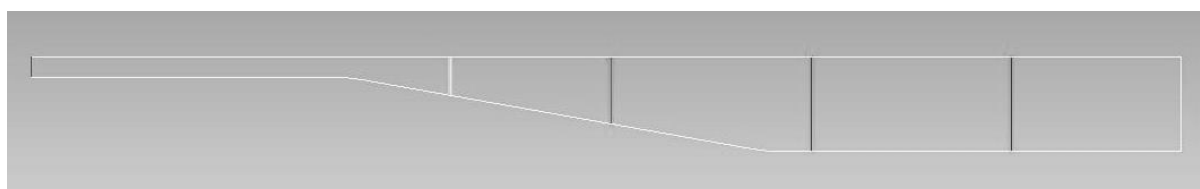


Fig. 14. Four different stations measured from expansion point throughout the 15H channel

From Figure 15, it can be seen that at station $x/H = 6$, trend of experimental results are quite similar to the solutions of k-epsilon turbulence model, but results of k-omega model are closest to the experimental results. Also, results of k-omega and SST k-omega turbulence models are almost same. In case of station $x/H = 14$ as showed in the Figure 16, solutions of all turbulence models are following the same trend which is similar to the experimental solutions; where results of both k-epsilon and k-omega turbulence models are closest to the experimental results.

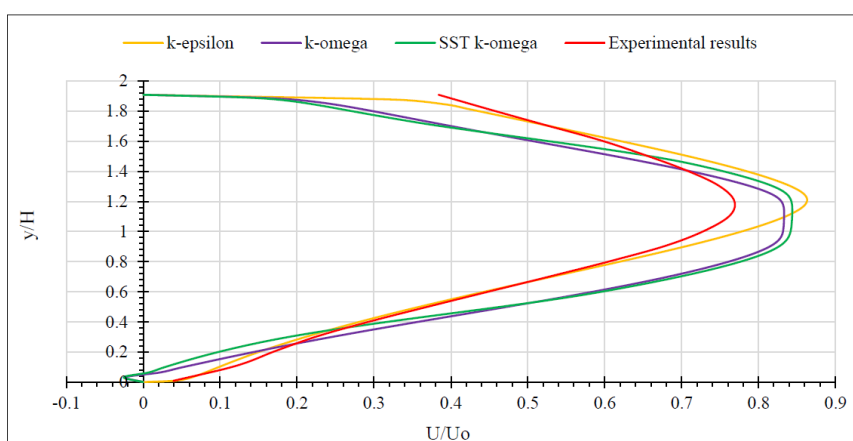


Fig. 15. 'y/H' versus 'U/U₀' for $x/H = 6$ (Model 1)

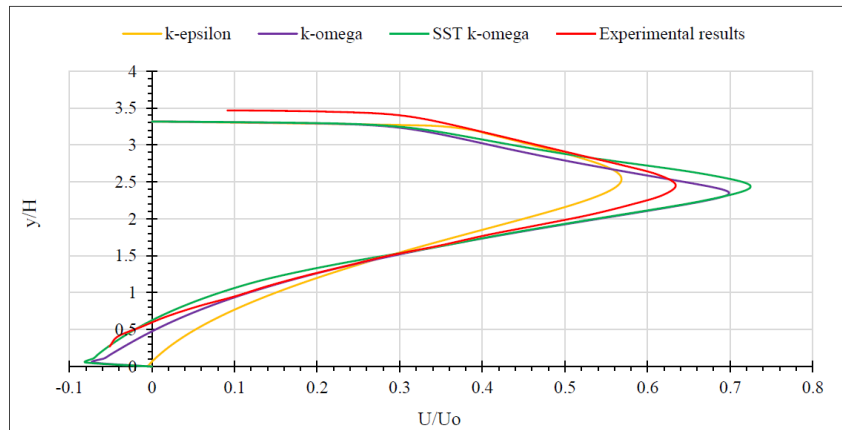


Fig. 16. y/H' versus ' U/U_o ' for $x/H = 14$ (Model 1)

As shown in Figure 17, at $x/H = 24$, trend of experimental results are quite similar to the solutions of k-omega and SST k-omega turbulence model; and results of k-omega turbulence model are closest to the experimental results. While, for curve length $x/H = 34$ as presented in the Figure 18, results of k-epsilon turbulence model are closest to the experimental results.

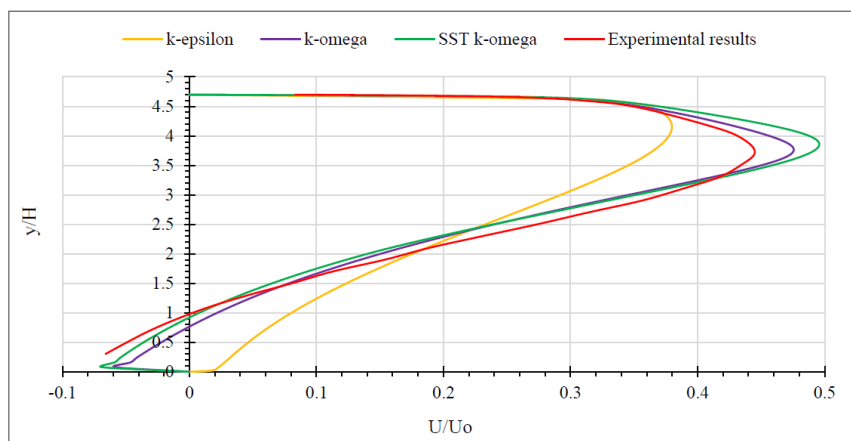


Fig. 17. ' y/H ' versus ' U/U_o ' for $x/H = 24$ (Model 1)

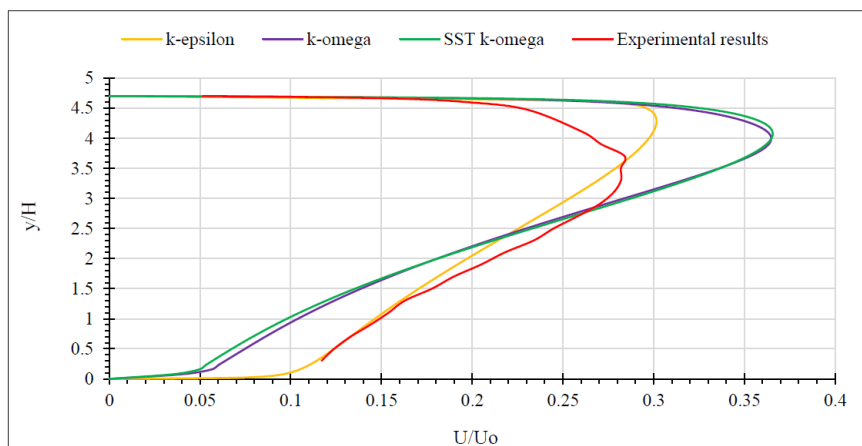


Fig. 18. ' y/H ' versus ' U/U_o ' for $x/H = 34$ (Model 1)

3.1.2 Analysis of model 2 (3H inlet channel)

Model 2 of the 2D symmetric diffuser was analyzed in the same way as model 1. It was analyzed using mesh B (168×60), for all three turbulence models - standard k-epsilon, standard k-omega and SST k-omega. The contours of x-velocity of these models is shown in Figure 19 to 21 showing velocity profiles and separations. From the figures it can be seen that- inlet of the diffuser possess higher velocity, but when flow goes out from the inlet channel there is an abrupt decrease in velocity creating turbulence, due to rapid increase in area and pressure in the diffuser. Which results in separation of boundary layer near the lower wall of the diffuser as the fluid flows towards x-direction. The negative velocity at the lower wall of the 2D asymmetric diffuser represents separation of boundary layer.

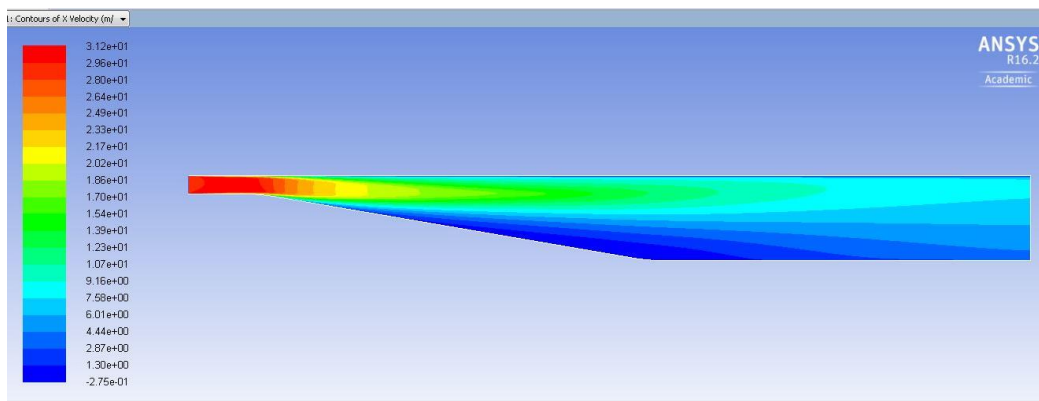


Fig. 19. Contours of X-velocity for the standard k-epsilon turbulence model

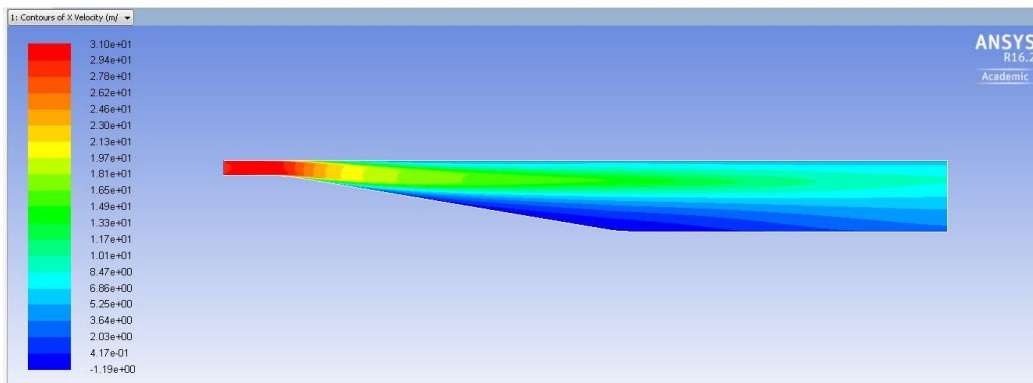


Fig. 20. Contours of X-velocity for the standard k-omega turbulence model

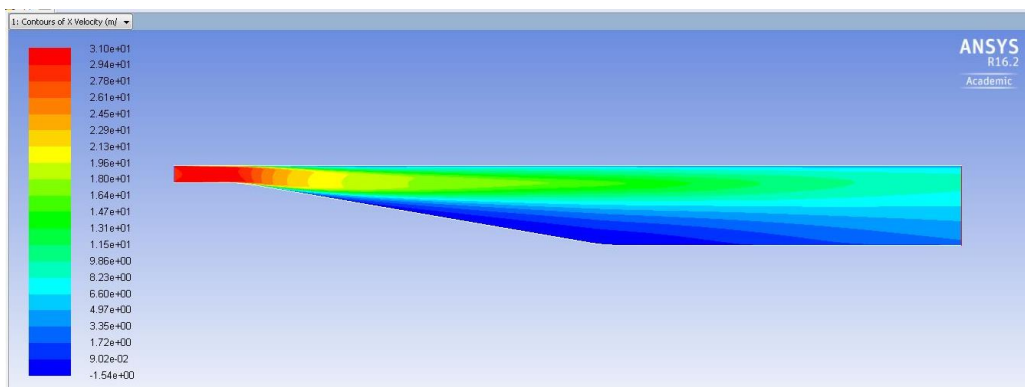


Fig. 21. Contours of X-velocity for the standard SST k-omega turbulence model

Figure 22 below represents the Y^+ values for different turbulence models namely standard k-epsilon, standard k-omega and SST k-omega of the 2D asymmetric diffuser model having inlet channel length $3H$. From the figure it is certain that standard k-omega and SST k-omega turbulence model possess lower wall Y^+ value as compared to standard k-epsilon turbulence model which is quite similar to model 1 with $15H$ inlet channel.

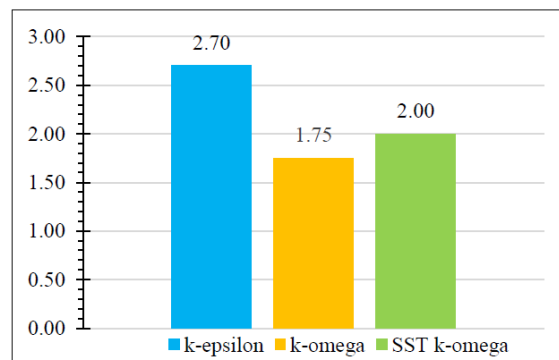


Fig. 22. Y^+ values for different turbulence model of Model 2

The ' U/U_o ' values at different stations viz. $x/H=6$, $x/H=14$, $x/H=24$ and $x/H=34$ measured from the expansion point (as shown in Figure 23) is compared to the different turbulence models and experimental results of the 2D asymmetric diffuser, and represented from the Figure 24 to 27 below.



Fig. 23. Four different stations measured from expansion point throughout Model 2

As shown in Figure 24, at curve length $x/H=6$, trend of experimental results are closest to the solutions of k-epsilon turbulence model. While, for curve length $x/H=14$ as presented in Figure 25, results of all the turbulence model are very similar to the experimental results; where solutions of SST k-omega turbulence model are nearest to the experimental results.

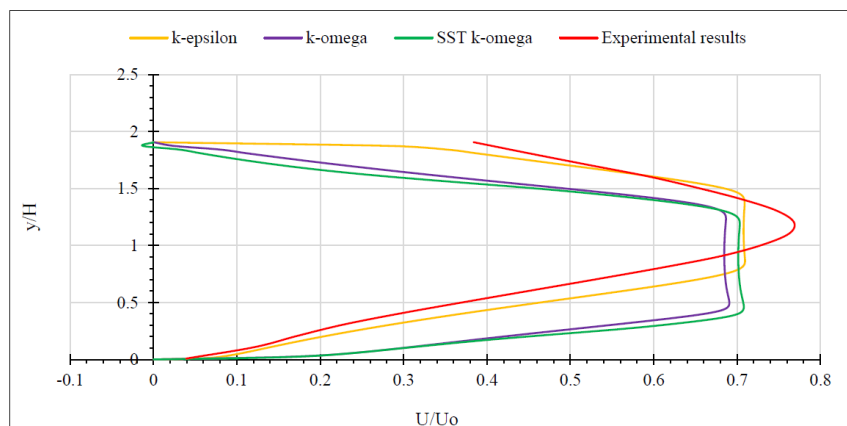


Fig. 24. ' y/H ' versus ' U/U_o ' for $x/H=6$ (Model 2)

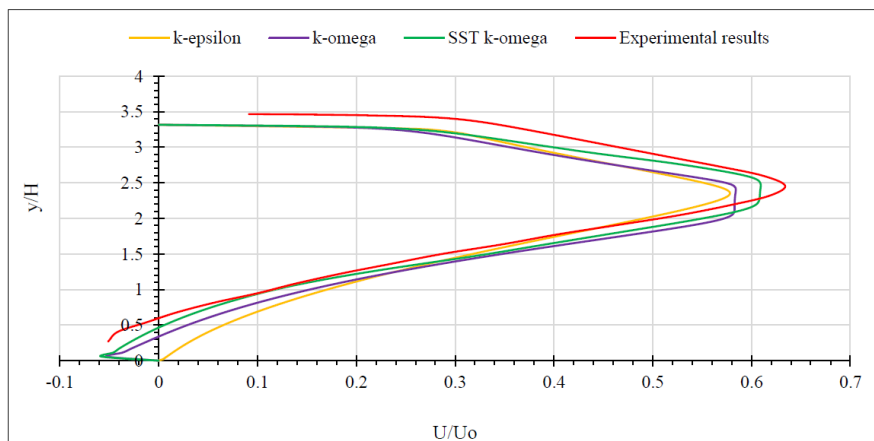


Fig. 25. 'y/H' versus 'U/Uo' for x/H = 14 (Model 2)

From Figure 26, at station x/H = 24, here all the turbulence model show quite comparable results with experimental results; while the trend of experimental results are closer to the solutions of both SST k-omega and k-epsilon turbulence models. On the other hand, for curve length x/H = 34 as presented in Figure 27, results of all the k-epsilon turbulence model are closest to the experimental results.

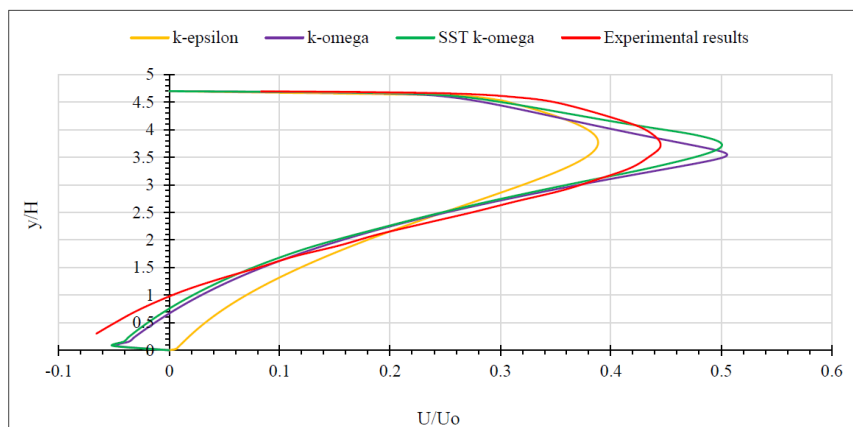


Fig. 26. 'y/H' versus 'U/Uo' for x/H = 24 (Model 2)

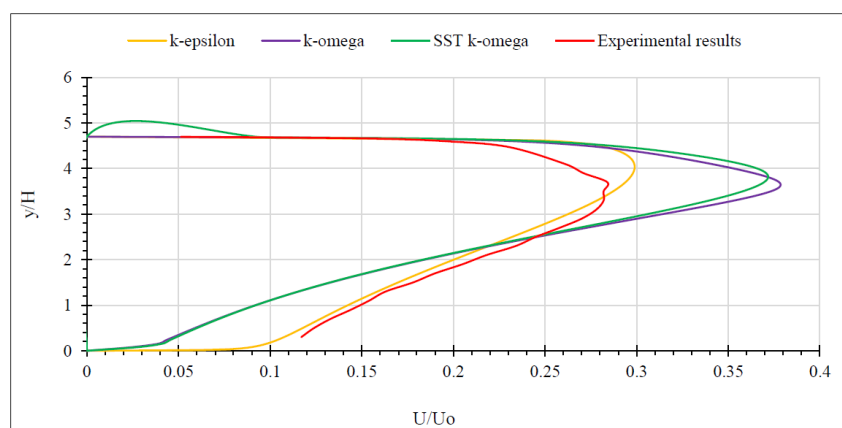


Fig. 27. 'y/H' versus 'U/Uo' for x/H = 34 (Model 2)

3.2 Comparison Between Model 1 And Model 2

From Figure 15 to 18, and Figure 24 to 27, it can be observed that in both model 1 and model 2 separation of boundary layer is more significant in stations $x/H = 14$, and $x/H = 24$. Also, in station $x/H = 34$ where flow is fully developed, the standard k-epsilon turbulence model shows better performance as compared to other turbulence models, while comparing with the experimental results. It is also important to note that, in most of the cases solutions of standard k-omega and SST k-omega turbulence models are very close to each other. Moreover, separation was under predicted by k-omega and SST k-omega in model 2 due to sudden decrease in flow velocity because of its shorter inlet channel length as compared to model 1.

The results obtained are consistent with the literatures of k-epsilon, k-omega and SST k-omega. K-epsilon models are good for fully turbulent flow away from boundary layers, but not good at capturing complex flows involving severe pressure gradient and separation. K-omega models have a better near wall treatment, and can predict the complex boundary layer flows such as flow in a diffuser, but they typically have an excessive and early prediction of flow separation. Similarly, SST k-omega which combines the capabilities of the k- ϵ model away from the walls and robustness of k-omega turbulence model near the walls.

While considering Y^+ values, k-epsilon turbulence model gives highest Y^+ values and k-omega turbulence model gives lowest Y^+ values in both the diffuser models. In brief, different turbulence models can be represented in decreasing order of Y^+ values as follows: k-epsilon > SST k-omega > k-omega.

4. Conclusion

The main objective of this study is the numerical study of an asymmetric 2D diffuser turbulent flow. In order to study separation and assess the effectiveness and consistency of different CFD turbulence models, primarily two models of asymmetric 2D diffuser were designed according to the given specifications. Then, mesh was generated and mesh independence study was carried out. After arriving at the independent mesh, the numerical study was carried out with different turbulence models viz. standard k-epsilon, k-omega and SST k-omega. Finally, solutions of different turbulence model obtained were compared with the experimental results.

From this entire study, the following conclusions were made:

- I. For both model 1 and model 2, 'k-epsilon' turbulence shows better performance at station $x/H = 34$.
- II. Separation of boundary layer is more significant in stations $x/H = 14$, and $x/H = 24$.
- III. Solutions of 'SST k-omega' and 'k-omega' turbulence models are almost same in all stations of the both diffuser models.
- IV. Separation was under predicted by k-omega and SST k-omega in model 2 due to sudden decrease in flow velocity because of its shorter inlet channel length as compared to model 1.
- V. Different turbulence models can be represented in terms of decreasing order of Y^+ values as follows : k-epsilon > SST k-omega > k-omega.

The differences between the numerical results and the experimental results are referring to the fact that the numerical results have numerical errors and those errors could come from many different sources, including the turbulence models.

Reasonably, this informal ranking of turbulence models is greatly dependent on the user and the information of interest. Nevertheless, these results have provided considerable insight into the capabilities of turbulence models which is indeed invaluable to figure out which CFD turbulent model can be used for an industrial engineering problem.

Acknowledgment

The authors would like to thank the Technicians at the Thermo Fluid Mechanics Research Centre University of Sussex for carrying out the experimental work used in validating the numerical results obtained.

Reference

- [1] Chang, Paul K. *Separation of flow*. Elsevier, 2014.
- [2] John David. *Introduction to Flight*. McGraw Hill, New York, USA, 2004.
- [3] Clancy, L.J. *Aerodynamics*. 1st Edition. John Wiley & Sons, New Jersey USA, 1975.
- [4] White, F.M. *Fluid Mechanics*. 7th Edition. McGraw Hill, New York, USA, 2010.
- [5] Cebeci, Tuncer, G. J. Mosinskis, and A. M. O. SMITH. "Calculation of separation points in incompressible turbulent flows." *Journal of Aircraft* 9, no. 9 (1972): 618-624.
- [6] Knob, M and Uruba, V. "Dynamics of Boundary Layer Separation". *Engineering Mechanics* 16, no. 1 (2009): 29–38.
- [7] Gustavsson, Jonas. "Experiments on Turbulent Flow Separation". *Master's thesis. Royal Institute of Technology Department of Mechanics*, (1998).
- [8] Yang, Zifeng, Fred Haan, Hui Hu, and Hongwei Ma. "An experimental investigation on the flow separation on a low-Reynolds-number airfoil." In *45th AIAA aerospace sciences meeting and exhibit*, (2007): 275.
- [9] Chandavari, Vinod, and Sanjeev Palekar. "Diffuser angle control to avoid flow separation." *International Journal of Technical Research and Applications* 2, no. 5 (2014): 16-21.
- [10] Törnblom, Olle, Astrid Herbst, and Arne V. Johansson. "Separation control in a plane asymmetric diffuser by means of streamwise vortices experiment, modelling and simulation." In *The 5th Symposium on Smart Control of Turbulence*, February. 2004.
- [11] Hashim, G.A., Wong, M.K., Sheng, L.C., and Azwadi, C.S. "Numerical Study of Turbulent Flow in Pipe with Sudden Expansion". *Journal of Advanced Research in Fluid Mechanics and Thermal Sciences* 6, no. 1. (2015): 34-48.
- [12] Berdanier, Reid A. "Turbulent flow through an asymmetric plane diffuser." *Masters Purdue University, West Lafayette, Indiana, US* (2011).
- [13] El-Behery, Samy M., and Mofreh H. Hamed "A Comparative Study of Turbulence Models Performance for Turbulent Flow in a Planar Asymmetric Diffuser". *World Academy of Science, Engineering and Technology International Journal of Aerospace and Mechanical Engineering* 3, no. 5 (2009).
- [14] Buice, Carl U., and John K. Eaton. "Experimental investigation of flow through an asymmetric plane diffuser." (1995).
- [15] Salehi, Saeed, Mehrdad Raisee, and M. J. Cervantes. "Computation of developing turbulent flow through a straight asymmetric diffuser with moderate adverse pressure gradient." *Journal of Applied Fluid Mechanics* 10, no. 4 (2017): 1029-1043.
- [16] Kumar, C and Kabbur, A.S. "Numerical Studies of a Two Dimensional Symmetric Diffuser in a Turbulent Flow Using CFD." *The Asian Review of Civil Engineering* 2, no. 2 (2013): 30-34.
- [17] Laccarino, Gianluca. "Predictions of a turbulent separated flow using commercial CFD codes." *Journal of Fluids Engineering* 123, no. 4 (2001): 819-828.
- [18] Jamil, M. M., M. I. Adamu, T. R. Ibrahim, and G. A. Hashim. "Numerical Study of Separation Length of Flow through Rectangular Channel with Baffle Plates." *Journal of Advanced Research Design* 7, no. 1 (2015): 19-33.
- [19] Saqr, Khalid M., Hossam S. Aly, Malzan A. Wahid, and Mohsin M. Sies. "Numerical simulation of confined vortex flow using a modified k-epsilon turbulence model." *CFD letters* 1, no. 2 (2010): 87-94.
- [20] Obi, S., K. Aoki, and S. Masuda. "Experimental and computational study of turbulent separating flow in an asymmetric plane diffuser." In *Ninth Symposium on Turbulent Shear Flows, Hyoto, Japan*, (1993): 305-1.
- [21] Klistafani, Y. "Experimental and Numerical Study of Turbulent Flow Characteristics in Assymmetric Diffuser". *International Conference ADRI - 5 Scientific Publications towards Global Competitive Higher Education*. (2017): 285-291.
- [22] Törnblom, Olle. "Experimental and computational studies of turbulent separating internal flows." PhD diss., KTH, 2006.

-
- [23] Pope, S. B. *Turbulent Flows*. 1st Edition. Cambridge University Press, Cambridge, United Kingdom, 2000.
- [24] Launder, Brian Edward, and Dudley Brian Spalding. "The Numerical Computation of Turbulent Flows". *Computer Methods in Applied Mechanics and Engineering* 3 (1974): 269-289.
- [25] Launder, Brian Edward, and B. I. Sharma. "Application of the energy-dissipation model of turbulence to the calculation of flow near a spinning disc." *Letters in heat and mass transfer* 1, no. 2 (1974): 131-137.
- [26] Wilcox, David C. *Turbulence modeling for CFD 2*. La Canada, CA: DCW industries, 1998.
- [27] Menter, Florian R. "Two-equation eddy-viscosity turbulence models for engineering applications." *AIAA journal* 32, no. 8 (1994): 1598-1605.
- [28] Ideen, S. "Mesh Generation in CFD: A Review". *CFD Open Series. Revision 1.75*, 2012.
- [29] Ghoreyshi, Mehdi, Jurgen Seidel, Keith Bergeron, Adam Jirasek, Andrew J. Lofthouse, and Russell M. Cummings. "Grid Quality and Resolution Effects on the Aerodynamic Modeling of Parachute Canopies." In *53rd AIAA Aerospace Sciences Meeting*, (2015): 04-07.
- [30] Versteeg, H. & K Malalasekera, W. "An Introduction to Computational Fluid Dynamics: The Finite Volume Method". *Longman Scientific & Technical*, (1995): 192-206.
- [31] Kaltenbach, H-J., M. Fatica, R. Mittal, T. S. Lund, and P. Moin. "Study of flow in a planar asymmetric diffuser using large-eddy simulation." *Journal of Fluid Mechanics* 390, (1999): 151-185.
- [32] Caretto, L. S., A. D. Gosman, S. V. Patankar, and D. B. Spalding. "Two calculation procedures for steady, three-dimensional flows with recirculation." In *Proceedings of the third international conference on numerical methods in fluid mechanics, Springer, Berlin, Heidelberg*, (1973): 60-68.
- [33] Patankar, Suhas V., and D. Brian Spalding. "A Calculation Procedure for Heat Mass and Momentum Transfer in Three Dimensional Parabolic Flows" *International Journal of Heat Mass Transfer* 15 (1972): 1787-1806.
- [34] Patankar, Suhas V. "A calculation procedure for two-dimensional elliptic situations." *Numerical heat transfer* 4, no. 4 (1981): 409-425.